

# A phenomenological approach to modelling collective cell movement in 2D

R. Rey · J. M. García-Aznar

Received: 1 May 2012 / Accepted: 13 December 2012 / Published online: 1 January 2013  
© Springer-Verlag Berlin Heidelberg 2012

**Abstract** There are two main approaches to unraveling the mechanisms involved in the regulation of collective cell movement. On the one hand, “in vitro” tests try to represent “in vivo” conditions. On the other hand, “in silico” tests aim to model this movement through the use of complex numerically implemented mathematical methods. This paper presents a simple cell-based mathematical model to represent the collective movement phenomena. This approach is used to better understand the different interactive forces which guide cell movement, focusing mainly on the role of the cell propulsion force with the substrate. Different applications are simulated for 2D cell cultures, wound healing, and collective cell movement in substrates with different degrees of stiffness. The model provides a plausible explanation of how cells work together in order to regulate their movement, showing the significant influence of the propulsive force exerted by the cell to the substrate on guiding the collective cell movement and its interplay with other cell forces.

**Keywords** Cell-based model · Cell movement · Numerical simulation · Tissue engineering

## 1 Introduction

Numerical simulation has normally been used as a tool for the simulation of both single-cell movement and collective cell migration (Jamali et al. 2010; Gracheva and Othmer 2004; Flaherty et al. 2007; Vermolen and Gefen 2012; Borau et al. 2011). The objective of these simulations is to improve the understanding of some experimental tests and to propose and

define new experiments to better understand collective cell movement and its organization in phenomena such as wound healing, tumor growth, or tissue formation.

These models can be mainly classified as continuum or discrete. Continuum models aim to describe the average behavior of cell populations with continuum variables. Thus, populations of cells are usually represented from a macroscopic point of view, without preserving the identity and properties of individual cells and underestimating the individual interaction between cells. Accordingly, cell movement evolution is described in terms of cell density and average velocities. This method has been applied for studying adhesion of different cell populations (Armstrong et al. 2006; Kopacz et al. 2008), cell spreading and wound healing (Arciero et al. 2011; Simpson et al. 2011), angiogenesis (Ambrosi et al. 2005), and other applications. Although these continuum models are less computationally expensive, their main drawbacks are that require more assumptions than discrete models, the individual movements of the cells cannot be tracked, and the behavior at the individual cell level cannot be predicted.

However, if cells are regarded as discrete elements with possible individual different features and interactions, the discrete particle method (Tijskens et al. 2003) appears as a clear paradigm for the numerical simulation of collective cell movement. This approach considers each cell to be defined as an individual, whose differences with the rest of the cells are due to position inside the group or tissue (Omelchenko et al. 2003), local chemical or mechanical environment (Tranquillo et al. 1988; Takebayashi et al. 1995; Kim et al. 2010; Pelham and Wang 1997), or other factors which could regulate cell behavior.

Following this approach, different methods have been proposed and used to investigate collective cell migration. Byrne and Drasdo (2009) studied the growing of cell

R. Rey (✉) · J. M. García-Aznar  
Mechanical Engineering Department, Aragon Institute of Engineering Research (I3A) (M2BE), University of Zaragoza, Zaragoza, Spain  
e-mail: rrey@unizar.es

colonies with an individual-based model which emphasizes cell to cell interaction with proliferation. Geris et al. (2010) reproduced skeletal tissue engineering, with cell apoptosis, growth, metabolism, and necrosis. Palsson and Othmer (2000) and Palsson (2001) presented the simulation of the collective movement of the *Dictyostelium discoideum*, including chemotaxis. Schaller and Meyer-Hermann (2007) showed a 3D model where the cells were represented by elastic spheres, with life cycles based on chemical interactions with the environment, but they did not consider any further mechanical interaction. Jamali et al. (2010) reproduced the internal cell structure by subcellular viscoelastic elements on growing epithelial cell culture. Vermolen and Gefen (2012) studied mechanical signaling among a colony of cells through the substrate by the strain energy field produced by the cells.

Although several cell-based models have been formulated, most them do not take into account the interaction of the cells with the substrate and the importance of this interaction in comparison with the other cell forces. One reason may be the scarce number of experimental tests of collective movement used to investigate the effect of substrate interaction on this migration. However, this effect has been widely investigated for individual cells as in Lo et al. (2000), Belousov et al. (2000), or Maruthamuthu et al. (2011). Indeed, new experimental techniques have been applied that allow estimation of the forces exerted by cells and their influence on the collective cell movement, as in Angelini et al. (2010, 2011), or Friedl and Wolf (2010).

The model presented here is used to represent different cell culture experiments in 2D, with the aim of trying to understand the emergent behavior of the cell population from single-cell interactive laws. Therefore, although this model is sufficiently general to include many different and complex effects (as have been used in other models), it is kept as simple as possible to be able to physically explain the experimental results. To evaluate the potential of our model, a number of “in silico” tests are simulated. These applications include a 2D monolayer expanding cell culture, a wound healing process, and a monolayer cell colony crossing the border between two substrates of different stiffness. Finally, some physically based conclusions are obtained combining the experimental data and the model, in order to better understand collective cell movement.

## 2 A discrete model to simulate cell migration

The proposed model is a discrete model based on individual cells, following the DEM (discrete element modeling) framework. The model comprises  $N$  cells, where every cell is assumed to have a spherical shape. Here, we simply assume that each cell is under the action of different forces where the cell sometimes plays an active role, whereas in other cases,

the cell simply plays a passive role. Note that we assume that all the forces are exerted on the center of the cell. For every cell  $i$ , it is necessary to fulfill the equilibrium condition.

$$\sum_{j=1}^N (\mathbf{F}_{ji,c-c}) + \mathbf{F}_{i,drag} + \mathbf{F}_{i,p} = 0, \quad \forall i = 1, \dots, N \quad (1)$$

where  $\mathbf{F}_{ji,c-c}$  represents the force that the  $j$  cell exerts on the  $i$  cell,  $\mathbf{F}_{i,drag}$  represents the drag force that the substrate exerts against the cell movement, and  $\mathbf{F}_{i,p}$  represents the reaction of the propulsion force that the  $i$  cell actively exerts on the substrate. All these forces and the cell radius may depend on different variables, such as the cell position, the cell type, the cell internal state, or other environmental factors. As a first approach, we assume the cell radius is kept constant.

### 2.1 Cell–cell interaction forces

Cell–cell interaction forces have different characteristics depending on the relative distance between the cells. If two cells are pressed together, they will repel each other due to the cytoskeleton and cytoplasm stiffness. However, when they are together and forced to separate, they will exert attraction forces due to chemical bonds created between their membranes. Therefore, we have assumed that cells are attracted due to mechano-chemical signals when they are close together.

In order to describe these characteristics, we model cell–cell interactions by means of the Morse potential (Newman (2005)). The force exerted by the cell  $j$  on the cell  $i$ , each cell with the position vector  $\mathbf{r}_i$ ,  $\mathbf{r}_j$  is represented as:

$$\mathbf{F}_{ji,c-c} = \left( A * \exp\left(-\frac{\|\mathbf{r}_j - \mathbf{r}_i\|}{\xi_1}\right) + B * \exp\left(-\frac{\|\mathbf{r}_j - \mathbf{r}_i\|}{\xi_2}\right) \right) * \frac{\mathbf{r}_j - \mathbf{r}_i}{\|\mathbf{r}_j - \mathbf{r}_i\|} \quad (2)$$

This distance-dependent model law represents three different zones. For  $\|\mathbf{r}_j - \mathbf{r}_i\| < R_0$ , the force will be positive (repulsive force), for  $\|\mathbf{r}_j - \mathbf{r}_i\| > R_0$ , the force will be negative (attraction force) with a maximum force  $F_{c-c,max}$ , and finally for  $\|\mathbf{r}_j - \mathbf{r}_i\| \rightarrow \infty$ , the force will decay and vanish (see Fig. 1). Finally,  $\xi_1$ ,  $\xi_2$ ,  $A$ , and  $B$  are functions depending on any internal cell variables or environmental parameters (see “Appendix A” and Table 1), although in this work, being a first approach, we consider these as constant parameters. Notice  $A < 0 < B$ .

### 2.2 Cell propulsion force

Cells interact with the ECM to propel themselves. This propulsion is exerted in “the polarization direction” of the cell, which represents the main direction in which the focal

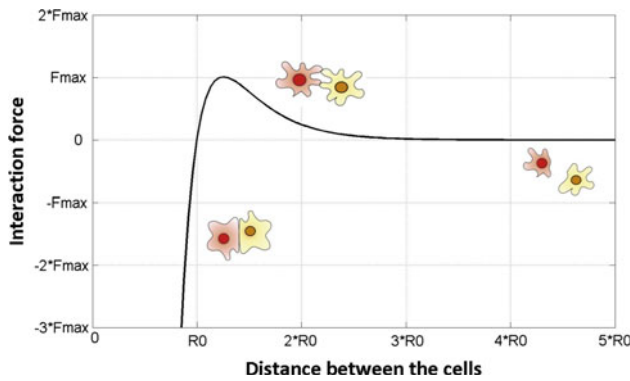


**Fig. 1** Cell–cell interaction force between two cells. *Negative values indicate repulsion.* Parameters of Eq. 2 can be adjusted to have the desired  $R_0$  (depending on the cell sizes,  $F_{c-c,max}$  or the decay rate for distances lower than  $R_0$ )

**Table 1** General parameters used in the model

Parameter	Value	Units
$A$	$-9.3184 \times 10^{-2}$	dyne
$B$	$6.10542 \times 10^{-3}$	dyne
$\xi_1$	2.94	$\mu\text{m}$
$\xi_2$	5.88	$\mu\text{m}$
$F_{c-c,max}$	$10^{-4}$	dyne
$\ \mathbf{F}_p\ $	$0 - 10^{-5}$	dyne
$f_d$	$10^4 * r_{cell}$	$\text{Ns}/\text{m}^2$
$r_{cell}$	16	$\mu\text{m}$

The parameters were chosen to be representative of the physical phenomenon which represents cell–cell attraction and repulsive forces

adhesion formation and cytoskeletal contractility propels the cell. The model represents this force ( $\mathbf{F}_{i,p}$ ) in the cell  $i$  as a combination of a force magnitude ( $\|\mathbf{F}_{i,p}\|$ ) and a cell-dependent polarization direction ( $\mathbf{p}$ ). The force magnitude follows the expression derived in Zaman et al. (2005), which depends on the ECM stiffness, the ligands density in the ECM, and different parameters depending on the internal chemistry of the cell. More details on the propulsion force modelization are given in ‘‘Appendix B’’. The influence of the external environment (mechanical or chemical) on the propulsion force magnitude can easily be included in this formulation. Nevertheless, for this work, we have considered only the influence of the substrate stiffness on the last application. The dependence of the propulsion on the other mentioned parameters (cell internal chemistry, substrate ligand density, etc.) is not considered, and the propulsion force magnitude is considered constant with respect to them. The propulsion direction follows the polarization vector stored for every cell. This polarization vector can be constant during the simulation time or variable depending on internal cell or external environmental variables. Nevertheless, in all

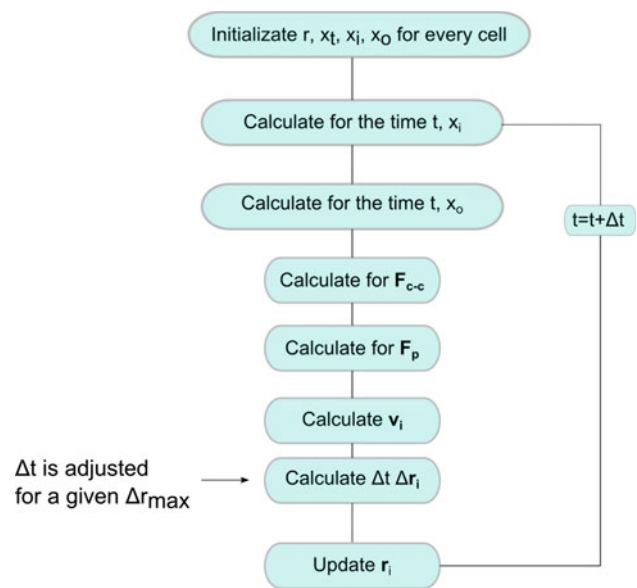


**Fig. 2** Numerical implementation scheme

the application examples simulated here, we assume these variables as constant in time.

### 2.3 Cell drag force

Cells are subject to a drag force which opposes their movement. Typically in 2D cultures, the cell rear focal adhesion must be deattached from the ECM to allow the cells to advance. In a 3D medium, similar drag forces are present with the addition of a viscous drag force which depends on both the ECM viscosity and its spatial structure. We assume a drag force depending on the velocity, following the same assumption as that presented by Zaman et al. (2005). Nevertheless, the constants that modulate the drag force may be dependent on the cell shape or size but also on any other internal or external cell parameter. In general

$$\mathbf{F}_{i,drag} = -f_d * \mathbf{v}_i \quad \forall i = 1, \dots, n \tag{3}$$

As a first approach in this work, we have considered  $f_d$  as a constant function equal to the viscous drag of a sphere in an infinitely viscous medium.

### 2.4 Numerical implementation

Figure 2 presents a scheme of the main steps followed for the numerical implementation of this model. The first step consists of the initialization of all the variables involved. In particular, it is necessary to define the initial distribution of the cells in the domain ( $\mathbf{r}_0$ ) consistent with their internal variables at the time zero. This initial definition is always difficult to determine (for example, the initial polarization) because it will depend on the previous history of every cell. The initial

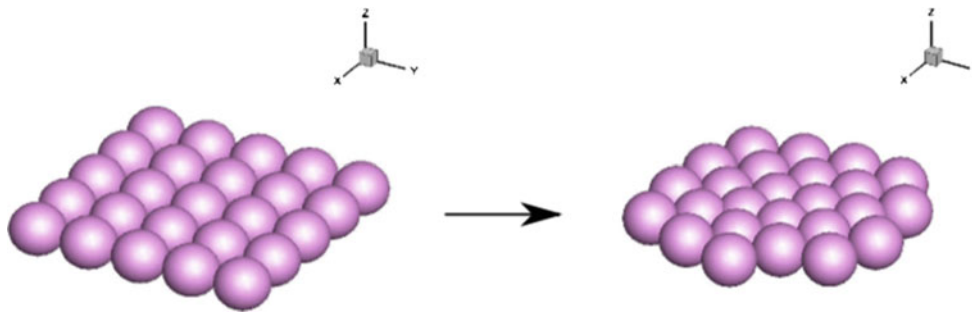


**Fig. 3** Cell initial seeding. In a similar manner to “in vitro” conditions, it is necessary to seed a cell configuration at the beginning of the analysis and let it evolve to achieve an initial equilibrium configuration.

This case shows an initial seeding in a square pattern that evolves in a “natural equilibrium” configuration after some numerical iterations

definition will thus depend on each particular simulation. It will normally be based on a common definition depending on the different cells type. Indeed, it should include some random distribution to simulate the nature variability of the cells.

Another important point is the initial position of every cell  $\mathbf{r}_0$  that has to be established at the beginning of the simulation. Therefore, the initial condition must represent some “real” configuration clearly depending on the application example. However, we have to keep in mind that any arbitrary configuration may not necessarily present a “natural equilibrium” state. For example, we can imagine the initial distribution of a monolayer cell colony. Cells initially placed very near or each other or with an initial ordered distribution will achieve a different equilibrium configuration, as can be seen in Fig. 3. Therefore, for each specific problem, it will be necessary, before starting the simulation, to evaluate an initial equilibrium configuration and afterward to simulate the conditions corresponding to each application.

Once this initial equilibrium condition is fully defined, explicit time integration iterations are started. The internal state variables of the cells are updated for the current time following their constitutive law, and after that environmental variables  $\mathbf{x}_o$  (stiffness, substrate ligand density, substrate chemical concentration, substrate stress state, etc.) are also updated. Once all the variables are updated, the different forces (cell–cell interaction, propulsive, and drag) are evaluated, and the equilibrium equation is solved to define the cell velocity.

The time integration is explicit because the highly non-linear nature of the problem makes an implicit method less attractive owing to the fact that it would need an inner iteration which would be computationally very expensive. Moreover, we use a first-order Euler approach. Again, a Runge–Kutta scheme or any other higher degree method would be computationally inefficient. However, to assure both stability and accuracy, it is necessary to control the

time step. This time step multiplied by the cell velocity must not produce a displacement greater than the smallest spatial scale of the problem. This spatial scale has been determined through the evolution of the cell repulsion force when two cells penetrate each other (see Fig. 1). Indeed, the time step is calculated to ensure that the maximum displacement is kept lower than a specific value (under 0.6 % of the cell radius), so the change in this force is small. The convergence was also checked by means of dividing the maximum allowed displacement by two and testing that does not produce changes to the numerical solution. This numerical implementation shows very good results and even solves the oscillating behavior reported in [Vermolen and Gefen \(2012\)](#).

### 3 Examples of application

#### 3.1 Expanding 2D monolayer cell cultures

2D cell cultures have previously been studied by “in vitro” tests, for example in [Huergo et al. \(2011\)](#), [Matsushita et al. \(1999\)](#), or [Trepap et al. \(2009\)](#). In fact, these cell cultures present an interesting field of study because of the different factors that allow to control the culture growth, the movement of the cells within or the cell internal organization. They therefore represent a suitable benchmark for testing our model on cell–cell interactive forces and substrate–cell forces. Indeed, the balance among these forces will dictate the deformation of the substrate under the culture expansion. In order to understand these interactions, the displacements on points of the substrate in the “in vitro” tests are usually measured ([Angelini et al. 2010](#)). In our model, the displacement field is determined by two contributing forces applied to substrate by the cells: the cell propulsive force (which not only reflects the propulsion magnitude, but also the polarization direction) and the drag force, on the negative direction of the cell speed (which in turn is influenced by the cell–cell

interaction in the force balance). The deformation pattern in the substrate is the result of the combination of force magnitudes, polarization direction, and cell movement guided by every force included in the model.

Secondly, we also aim to study the influence of the spatial ordering of the polarization direction of the cells on the internal stress state of the cells. Internal stresses in a cell sheet can be deduced from other experimental data or estimated from numerical simulations. In fact, Tambe et al. (2011) or Trepap and Fredberg (2011) use MSM (monolayer stress microscopy), which starts with the interaction forces at the cell–substrate interface of a monolayer cell sheet and then uses a straightforward balance of forces to measure the distribution of physical forces at every point within that monolayer. Nevertheless, internal stresses in the cell monolayer sheet are important because they provide insights into which regulatory mechanism drives the colony expansion: the pulling of the outer edge cells or the internal pushing of the growing internal cells, or even other factors. Thus, following the experimental results of Trepap et al. (2009) which show that stresses inside a canine kidney cell sheet are positive, we simulate a similar colony with two different polarization patterns in the cell culture. One pattern is random where the polarization direction is defined randomly at the beginning of the simulation and the second pattern is simulated considering every cell polarized in a radial outward direction departing from the culture center. Other polarization patterns could be simulated as an unidirectional pattern with every cell moving in the same direction.

Both cell cultures are simulated by a 2D cell distribution with 3,200 cells using the model parameters indicated in Table 1. The initial spatial definition comes from the free evolution of the cell colony initially placed in a radial symmetry configuration and perturbed by random-oriented propulsion forces of small magnitude. The colony evolves naturally to another disordered natural configuration which is taken as the geometrical initial configuration.

### 3.2 Wound healing

The healing of a wound is simulated in a cell monolayer with a circular shape of different sizes. The “undamaged tissue” is a layer of 3,200 cells in a steady configuration with the parameters shown in Table 1. The initial spatial configuration is equal to that used in the previous application example. Different numbers of cells are removed from the central part of the culture in order to simulate a wound of 700 and 2,500  $\mu\text{m}^2$  size. We then continue with the simulation in order to observe how the cell colony reacts to this wound.

We study the influence of the different forces on the wound healing speed. Two different approaches are considered to simulate the cell behavior. Firstly, a pure epithelial behavior is simulated. In this case, we consider that no propul-

sion forces are exerted by the cells on the ECM and that the movement is mainly regulated by cell–cell interaction. Secondly, however, we consider that cells use the ECM to propel themselves. A propulsion force appears with the polarization vector pointing inside the wound. These results are compared with the experimental tests performed by Grasso et al. (2007) in bovine corneal endothelial-induced wounds with and without ECM (with or without cell propelling forces).

### 3.3 Collective cell movement across an interface with stiffness change

Lo et al. (2000) showed that individual fibroblast movement was affected by substrate stiffness. Single fibroblasts were able to cross the border between a soft and a rigid substrate material, but not in the contrary direction. Nevertheless, we propose here to investigate, from a theoretical point of view what would happen if instead of a single cell, a whole cell colony tried to cross the stiffness border.

A colony of 1,500 cells with propulsion capacity (such as an epithelial cell sheet Friedl et al. (2004)) has been simulated, with its polarization vector always pointing to the right. The general model parameters are stated in Table 1. We consider that there is a change in material stiffness at  $X = 0$ . Two studied cases are studied: case a) from a stiff material ( $E = 100$  kdyn/cm<sup>2</sup>, left side) to a soft material (1 kdyn/cm<sup>2</sup>, right side) and case b) from a soft material ( $E = 1$  kdyn/cm<sup>2</sup>, left side) to a stiff material (100 kdyn/cm<sup>2</sup>, right side).

For this specific example, we consider that the propulsion force  $\|\mathbf{F}_p\|$  depends on the substrate stiffness (as has also been shown in Lin et al. (2010)), according to the law originally posed by Zaman et al. (2005).

$$\|\mathbf{F}_p\| = \begin{cases} F_{p,\max}, & \text{if } E_{\text{substrate}} \geq 100,000 \text{ Pa} \\ F_{p,\max} * \frac{E_{\text{substrate}}}{1e5}, & \text{if } E_{\text{substrate}} \leq 100,000 \text{ Pa} \end{cases} \quad (4)$$

Finally, we also study the influence of the value of  $F_{p,\max}$  with respect to the maximum force of attraction among cells,  $F_{c-c,\max}$ , and how this balance regulates the colony behaviour. Therefore, for every substrate configuration, two different force ratios are studied:  $F_{p,\max} = 10\% * F_{c-c,\max}$  and  $F_{p,\max} = F_{c-c,\max}$ .

## 4 Results and discussion

### 4.1 Expanding 2D monolayer cell cultures

The objective of the simulation is to see whether the model is able to predict cell–material interaction of the different forces in the cell colony during its expansion. To facilitate comparison with experimental results, we have considered

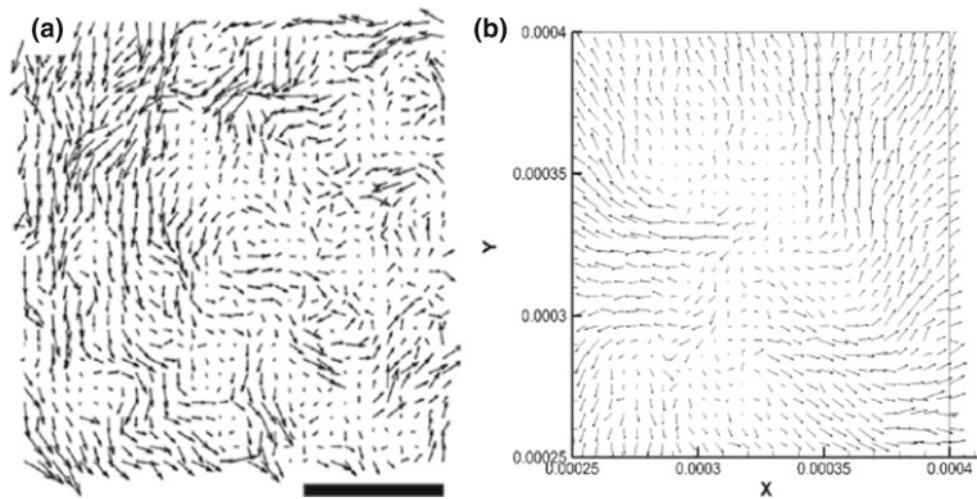


**Fig. 4** Fields of the substrate displacement obtained **a** from Angelini et al. (2010) (reproduced with permission) and **b** from the monolayer cell sheet simulation. The *vectors* show the direction and relative magnitude of the displacement in the substrate

the results presented in Angelini et al. (2010), where the authors extract the deformation of the ECM by means of a large group of seeded cells. The deformation pattern of the substrate is obtained by the TFM (traction force microscopy) technique (Benigno et al. 2002).

As our method can distinguish among the different forces that regulate cell movement inside the colony, it is possible to perform the inverse process of the analysis normally developed in TFM. We numerically obtain the displacements in the substrate by applying the forces on it from the cells recovered from the simulation and obtaining the displacement field by the Boussinesq equation. In this way, we obtain an image from our calculated displacement field and we can easily establish a comparison. Figure 4 shows two images, one from our simulation and the other from Angelini et al. (2010). The displacement field is the result for the cell–substrate interaction that in our model comprises the drag force and the propulsion force, each based on its own proposed model. Both images show swirl displacement patterns under the cell sheet.

We see from our simulations that the forces involved in collective cell movement are able to represent, at least qualitatively, the interaction of the forces with the substrate. Normally forces from the cells to the substrate are studied in terms of cell spreading (Zemel et al. 2010) or distributed in the cell perimeter as in Buxboim et al. (2010). It is not as usual, especially in 2D cultures, to study the substrate–cell forces separately in two different contributions (propulsion and drag proportional to the cell velocity) as we have described in our model. Nevertheless, the comparison with Angelini et al. (2010) shows that it is possible to unify the source of the drag in both 2D and 3D studies, simulating it in the same direction as the cell velocity.



**Fig. 5** The figure represents the cells in the colony border with a vector representing the cell–cell internal resultant in every cell. *Dotted lines* represent different rows (*first, second, and third*) from the colony outer edge. The cell–cell internal force is calculated in every cell, projected to the curve normal pointing inward and this projection average along 20 cells

We are also able to obtain the stress state inside the cell sheet. We identify the outer border of the colony and we identify twenty cells in this border. We calculate the curve which represents this border and the vector normal to this curve pointing inward to the colony ( $\mathbf{n}$ ). Then, we evaluate the average cell–cell force component pointing inward.  $F_{av} = \frac{1}{20} \sum_{i=1}^{20} \mathbf{F}_{c-c,i} \cdot \mathbf{n}_i$ . The same process is repeated for the next twenty cells that form the second row on the outer part of the colony and so for eight different rows (see Fig. 5). Finally, these forces are represented as stresses by dividing by the cell diameter (16  $\mu\text{m}$ ) and the assumed cell height (5  $\mu\text{m}$ ). This method is very similar to that used by Trepat et al. (2009) with the difference that these authors calculated the cell–cell force indirectly by means of the cell–substrate deformation while our numerical simulation allows the evaluation of these cell–cell forces directly.

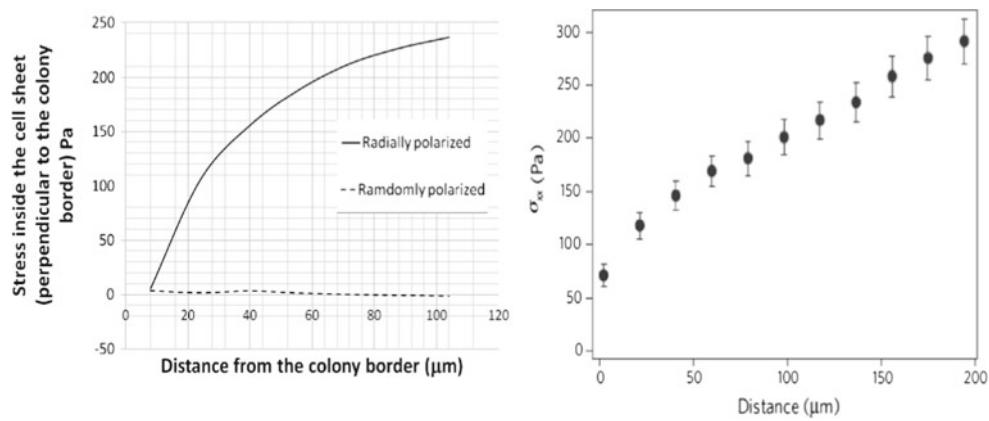


**Fig. 6** Stresses in the cell sheet obtained in the simulation with radial polarization pointing outwards and with randomly polarization distribution (left) and in the experimental results obtained by Trepap et al. (2009) (right) (reproduced with permission)

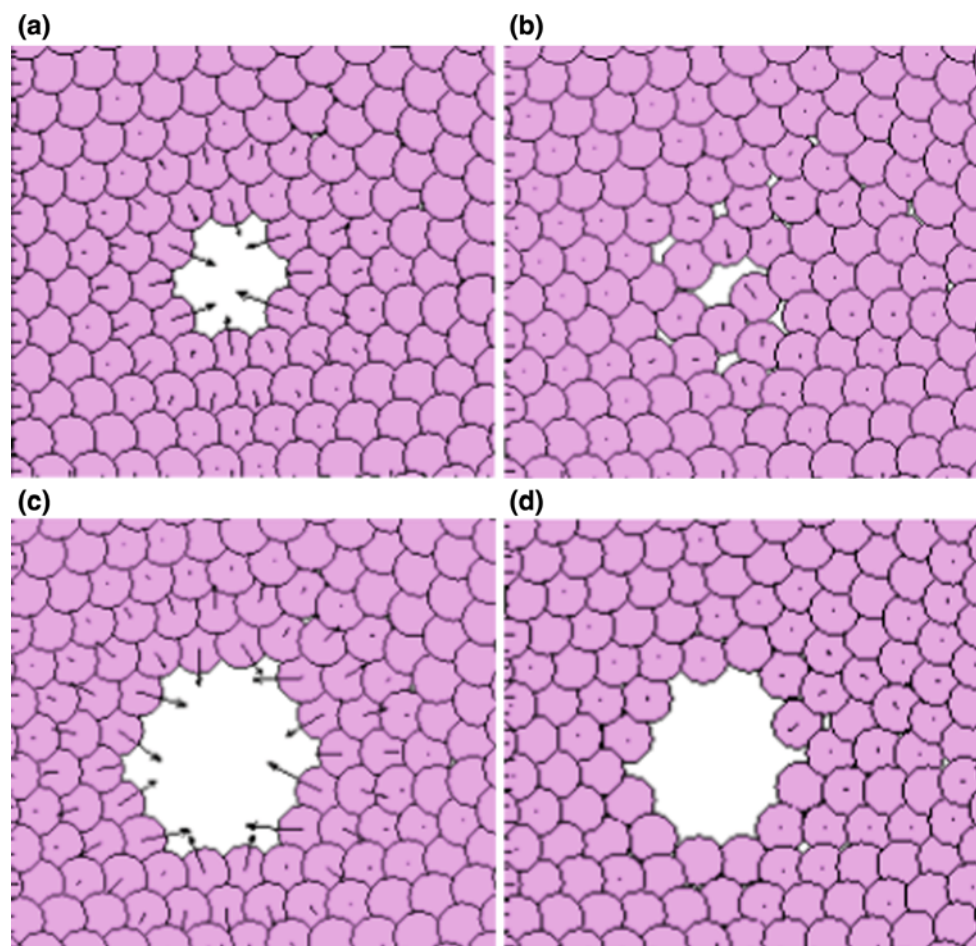


**Fig. 7** Temporal evolution of the healing of the wound for the **a** small (700  $\mu\text{m}^2$ ) and the **c** large (2,500  $\mu\text{m}^2$ ) wound size at the start of the wound closing and **b** after 30 min for the small initial wound and **d**

after 60 min for the larger initial wound. The images are taken from simulation without propulsive forces exerted by the cells. The vector represents the resultant of the cell–cell interaction forces

The results for the two assumed polarization patterns (random and radial outward direction) are shown in Fig. 6, together with the experimental results. After obtaining the

stresses inside the cell sheet for the two assumed polarization patterns, we have also been able to corroborate the conclusion extracted from the experiments in Trepap et al. (2009), which

points to a net tension state inside the cell sheet. If a 2D colony shows an internal tension stress state, it is because there is a net tendency of the cells in the colony to move radially outward (polarization of propulsion forces points outwards from the colony). We also confirm that if the polarization of propulsion forces of the cells is randomly oriented, the stresses inside the sheet do not grow on tension, but even decrease and becoming compressive in the central part of the colony.

The fundamental mechanisms that regulate this behavior are still unexplained. One hypothesis is that border cells could have contact inhibition of the migration (Carmona-Fontaine et al. 2008) that makes the propulsion polarization point away from the other cells. This could partially explain the net tension stress inside the cell sheet, but does not explain the radial polarization of the cells placed inside the colony. Another hypothetical explanation could be that the polarization direction depends on the resultant cell–cell forces that one individual cell can sense and that the propulsion polarization tries to align with these resultant forces.

#### 4.2 Wound healing

Differences in wound healing speed depending on the ECM stiffness and resultant propelling forces are studied. The simulation determines the behavior of the cells adjacent to the wound and the evolution of their mechanical state during the different healing stages. The resulting cell–cell forces for every cell are shown in Fig. 7.

For different wound sizes, it can be seen that at the beginning of the simulation, the healing starts due to the equilibrium rupture of the cell colony provoked by the wound. In a non-damaged colony, the cells achieve an equilibrium of forces. When some cells are removed and the wound is initiated, cells around the wound border have a resultant cell–cell force that impels them to move, filling the wound. The healing begins due to the force imbalance. After a few minutes, the new configuration reduces this imbalance of cell–cell forces and a different bias appears. If the wound is small, the healing speed is maintained because the cells at the opposite sides of the wound begin to influence each other. If not, the speed of the wound healing is reduced. Under these conditions, the propelling forces exerted by the cells on the ECM are very significant. If the cells start to produce protrusion from the actin polymerization at the edge of the wound, the propulsion will start in the polarization direction and the wound healing speed will be maintained. On other hand, if there is not cell propulsion, the wound still closes slowly because the cell–cell interaction forces produce a contractile ring that pulls the wound edge together. Figure 8 shows the evolution of the wound area over the time and the two different cell behavior (with and without propelling force) for the two wound sizes. Finally, it must be emphasized that we do

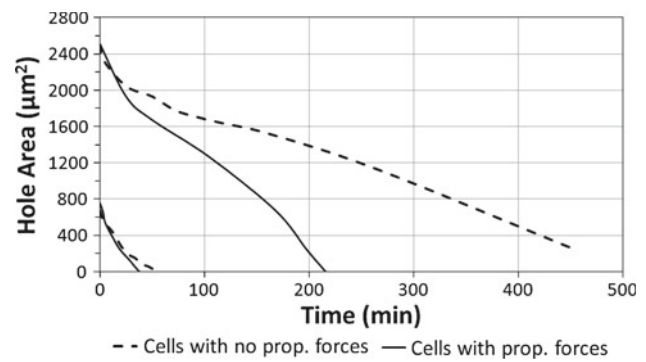


**Fig. 8** Time evolution of the wound area is shown with the two different assumptions that cells have or do not have propulsive forces. Two initial wound areas are studied

not imply that only cell–cell interaction forces alone can heal any wound size. If the initial wound size is large enough, no influence will appear between the wound opposite sides of the wound and the healing time will be extremely long.

It is important to note that this behavior is qualitatively similar to experimental data on wound healing closure. The difference in the healing mechanism between propelling cells and non-propelling cells was reported in Bement et al. (1993) and extensively studied in Grasso et al. (2007). In this latter study, very similar results to our simulation are reported. Healing speeds are similar in the first instant of the healing with or without ECM, but the speed subsequently reduces if the cells cannot propel themselves interacting with the ECM.

#### 4.3 Collective cell movement across an interface with stiffness change

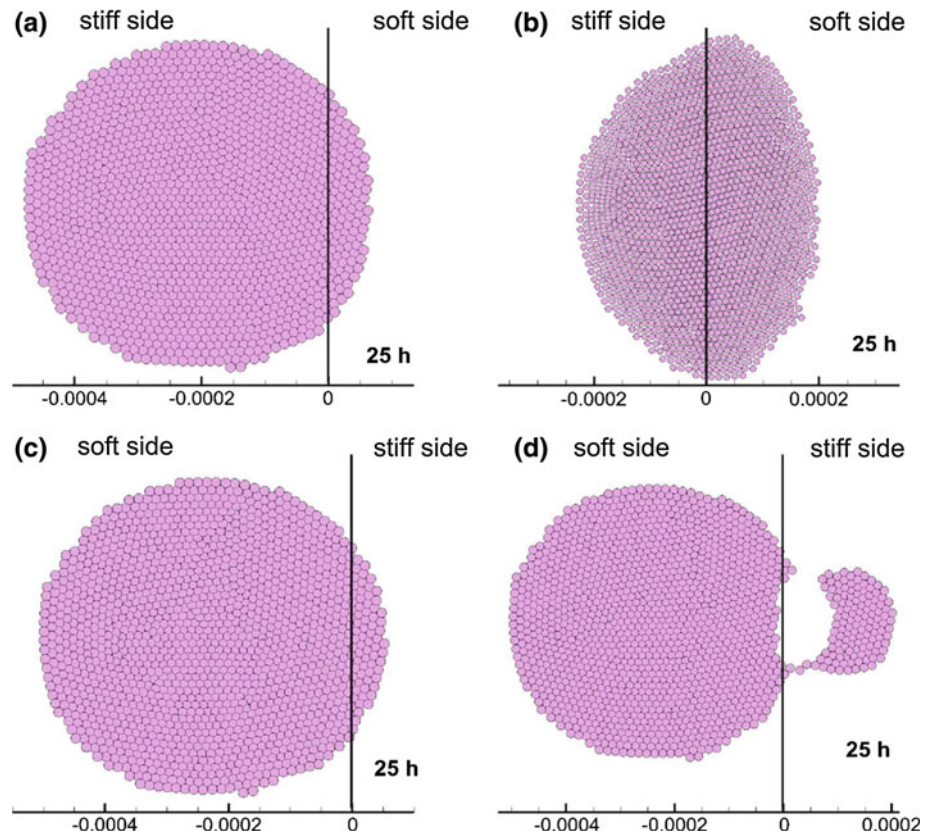
Figure 9 shows the numerical results for collective cell movement crossing interfaces between materials with different degrees of stiffness. The cells move from left to right and different final movement patterns appear depending on the relation between the stiffness. The simulated time is typically around 1 day of cell life.

The influence of the ECM stiffness on the single-cell migratory speed has already been studied and measured [(as in Discher et al. (2005) or Lo et al. (2000)] and also whether or not an individual cell is able to cross a stiffness discontinuity in the substrate. We have simulated this experiment with a colony instead of a single cell with a unidirectional collective motion (induced numerically simulating, for example, chemotaxis).

Our numerical simulations provide additional information about plausible mechanisms that could regulate collective cell movement around one interface with a strong variation in the rigidity. When the colony crosses from the stiff to the soft side, the rear cells still remaining in the stiff part continue pushing the colony and the colony is able to cross the border.



**Fig. 9** Time evolution of cell configurations during collective movement. **a** and **b** represent the culture moving leftwards from stiff ECM to soft ECM. **c** and **d** represent the culture moving rightwards from soft ECM to stiff ECM. **a** and **c** has  $\|\mathbf{F}_{i,p}\| = 10\% * F_{c-c,max}$  and **b** and **d**  $\|\mathbf{F}_{i,p}\| = F_{c-c,max}$



In addition, the initial circular configuration is deformed and the cells form a much more ellipsoidal shape if the propulsion force is similar to the maximum cell–cell interaction force.

This collective movement is completely different from the individual cell movement, where the single cell is nearly stopped because it lacks the pushing effect from the rear cell partners. When the colony crosses from the soft to the stiff side, the cells in the stiff part begin to pull the cells still in the soft part. In this case, the ratio between the propulsion force level and the maximum cell–cell interaction force is very significant. If the forces are very similar, the cells in the stiff part of the ECM can surpass the maximum cell–cell attraction force and detach themselves, leaving the colony in the soft part.

## 5 Conclusion

The model presented here has been shown useful to represent different mechano-biological tests improving the knowledge of the involved mechanisms in collective cell migration. Nevertheless, it should be borne in mind that this is a first approach that has some limitations requiring further discussion. Firstly, the addition of further biological effects, such as cell proliferation (Evan and Vousden

2001), matrix production, and degradation (Raeber et al. 2005), (Stylianopoulos and Barocas 2007), the life cycle, or death of the cells [(simulated in other works such as (Geris et al. 2010)] could improve our current model. Secondly, the proposed model uses a very simple approach to describe mechanical interactions. A better mechanical representation of cell behavior could be simulated by including viscoelastic effects in the cell–cell interaction due to the cytoplasm (Palsson 2001) and cell–material interaction via mechanosensing mechanisms (Reinhart-King et al. 2008; Borau et al. 2011). Finally, chemical intracellular and intercellular signaling mechanisms could also affect the phenomena and should be at least partially included in the model.

Nevertheless, these simplifications do not affect the conclusions of this work. We have hypothesized different physical assumptions and defined a simple model that helps to understand the force interaction among cells and especially the interaction of the cells with the substrate. In particular, we have investigated how cell propulsion polarity plays a critical role in the regulation of collective cell movement and how substrate stiffness affects collective cell movement by regulation of the propulsion force magnitude. We have shown the relevance of these cell–substrate forces, not only in terms of their existence, but also in terms of their magnitude relative to other forces.

**Acknowledgments** We are grateful to Dr. Trepal and Dr. Angelini for useful and enlightening discussions. This research was supported by the Spanish Ministry of Science and Innovation (DPI 2009-14115-CO3-01) (project part financed by the European Union, European Regional Development Fund).

## 6 Appendix A: Relation between Morse potential mechanical parameters and mathematical parameters

As described in the text, the cell–cell interaction force is represented by a Morse potential:

$$\mathbf{F}_{j,i,c-c} = \left( A * \exp\left(-\frac{\|\mathbf{r}_j - \mathbf{r}_i\|}{\xi_1}\right) + B * \exp\left(-\frac{\|\mathbf{r}_j - \mathbf{r}_i\|}{\xi_2}\right) \right) * \frac{\mathbf{r}_j - \mathbf{r}_i}{\|\mathbf{r}_j - \mathbf{r}_i\|} \quad (5)$$

This formulation depends mathematically on four parameters:  $A$ ,  $B$ ,  $\xi_1$  and  $\xi_2$ . However, in terms of test correlation or physical understanding different parameters have been selected. It is necessary to choose four parameter to get a full determined set of equation. But physically selected parameters can not be parameters as easily declared as linear stiffness or attraction force because function shape is more complex than that. So the following parameters have been selected to fully represented the function shape:

- $R_0$  represents the distance between two cells that implies change in the interaction force between repulsion and attraction. This has been selected as the cell radius, with a value of 16  $\mu\text{m}$ .
- $F_{\max}$  represents the maximum attraction force between the two cells. This will be produced at a cell–cell distance of  $R_1$ . The maximum attraction has been selected as  $10^{-4}$  dyne.
- $FR_1$  The ratio between the repulsion force at 80 %  $R_0$  and  $F_{\max}$ . 500 % has been selected.
- $FR_2$  The ratio between the attraction force at  $R_0 + (R_1 - R_0)/4$  and  $F_{\max}$ . 23 % has been selected

Now it is necessary to pass from mechanical or physical parameters to mathematical parameters. The following equations are established:

$$\left( A * \exp\left(-\frac{R_0}{\xi_1}\right) + B * \exp\left(-\frac{R_0}{\xi_2}\right) \right) = 0 \quad (6)$$

$R_1$  such as

$$\frac{\partial \left( A * \exp\left(-\frac{R_1}{\xi_1}\right) + B * \exp\left(-\frac{R_1}{\xi_2}\right) \right)}{\partial r} = 0 \quad (7)$$

$$F_{\max} = \left( A * \exp\left(-\frac{R_1}{\xi_1}\right) + B * \exp\left(-\frac{R_1}{\xi_2}\right) \right) \quad (8)$$

$$FR_1 = \frac{\left( A * \exp\left(-\frac{80 \% R_0}{\xi_1}\right) + B * \exp\left(-\frac{80 \% R_0}{\xi_2}\right) \right)}{\left( A * \exp\left(-\frac{R_0}{\xi_1}\right) + B * \exp\left(-\frac{R_0}{\xi_2}\right) \right)} \quad (9)$$

$$FR_2 = \frac{\left( A * \exp\left(-\frac{R_0 + (R_1 - R_0) * 4}{\xi_1}\right) + B * \exp\left(-\frac{R_0 + (R_1 - R_0) * 4}{\xi_2}\right) \right)}{\left( A * \exp\left(-\frac{R_0}{\xi_1}\right) + B * \exp\left(-\frac{R_0}{\xi_2}\right) \right)} \quad (10)$$

It is not possible to calculate this set of equations explicitly, so they are calculated by a Newton-Raphson iterative process.

The explained four physical parameters explained above determine the relation between the interaction force and the distance between the cell. We will now compare the proposed quantitative relation with measured data. It must be remarked that this relation is not easily measured. [Helenius et al. \(2008\)](#) uses atomic force microscopy (AFM) for single-cell force spectroscopy (SCFS). It extracts a force–cell distance relation similar on shape to the relation obtained from the Morse potential, with a maximum attraction force very close to  $10^{-4}$  dyne, the value selected for this work.

Other measured parameter that can be compared with our relation values is the local stiffness derived from the third parameter chosen. The repulsion force at 80 %  $R_0$  derives a local stiffness of 1.5 nN/ $\mu\text{m}$ . This value is inside the range measured with atomic force microscopy (AFM) in [Hayashi \(2006\)](#).

## 7 Appendix B: Zaman's formulation for cell propulsive force on 3D

[Zaman et al. \(2005\)](#) develop a computational model for cell migration in 3D matrices using a force-based dynamics approach. The relation between the propulsion force and internal cell parameters or external environmental parameters used on this work has been based on that reference.

In particular, the cell propulsion force modulus of a  $i$  cell ( $F_{i,p}$ ) is described as the product of the force per ligand–receptor complex ( $F_{R,L}$ ) by a dimensionless parameter measuring the binding strength of the receptors to the ligands in the ECM ( $\beta_f$ ).

$$F_{i,p} = F_{R,L} * \beta_f \quad (11)$$

In addition,  $F_{R,L}$  is assumed to vary directly with the ECM Young's Modulus up to a certain value of Young's Modulus and then saturates with further increase in ECM stiffness.

The hypothesized model is completed with the definition of  $\beta_f$  as

$$\beta_f = k_1 * n_f * [L_f]; \quad (12)$$

with  $k_1$  the binding constant for the binding of integrins at the front end of the cell to the ligands in the ECM (in  $M^{-1}$ ),  $n_f$  the total number of available receptors on the front part of the cell and  $[L_f]$  the concentration of the ligands at the leading edge of the cell in the ECM (in M).

Finally it must be remarked that for this work we have considered only the influence of the substrate stiffness on the last application. The dependence of the propulsion on the other mentioned parameters (cell internal chemistry, substrate ligand density, etc.) are not considered and the propulsion force magnitude is considered constant with respect to them.

## References

- Ambrosi D, Gamba A, Serini G (2005) Cell directional persistence and chemotaxis in vascular morphogenesis (vol 66, pg 1851, 2004). *Bull Math Biol* 67(1):195
- Angelini TE, Hannezo E, Trepast X, Fredberg JJ, Weitz DA (2010) Cell migration driven by cooperative substrate deformation patterns. *Phys Rev Lett* 104(16):168104
- Angelini TE, Hannezo E, Trepast X, Marquez M, Fredberg JJ, Weitz DA (2011) Glass-like dynamics of collective cell migration. *Proc Natl Acad Sci USA* 108(12):4714–4719
- Arciero JC, Mi Q, Branca MF, Hackam DJ, Swigon D (2011) Continuum model of collective cell migration in wound healing and colony expansion. *Biophys J* 100(3):535–543
- Armstrong NJ, Painter KJ, Sherratt JA (2006) A continuum approach to modelling cell-cell adhesion. *J Theor Biol* 243(1):98–113
- Belousov L, Louchinskaia N, Stein A (2000) Tension-dependent collective cell movements in the early gastrula ectoderm of *Xenopus laevis* embryos. *Dev Genes Evol* 210(2):92–104
- Bement W, Forscher P, Mooseker M (1993) A novel cytoskeletal structure involved in purse string wound closure and cell polarity maintenance. *J Cell Biol* 121(3):565–578
- Beningo KA, Lo C-M, Wang Y-L (2002) Flexible polyacrylamide substrata for the analysis of mechanical interactions at cell-substratum adhesions. *Method Cell Biol* 69:325–339
- Borau C, Kamm RD, Garcia-Aznar JM (2011) Mechano-sensing and cell migration: a 3d model approach. *Phys Biol* 8(6):1078–1088
- Buxboim A, Ivanovska IL, Discher DE (2010) Matrix elasticity, cytoskeletal forces and physics of the nucleus: how deeply do cells 'feel' outside and in? *J Cell Sci* 123(3):297–308
- Byrne H, Drasdo D (2009) Individual-based and continuum models of growing cell populations: a comparison. *J Math Biol* 58:657–687
- Carmona-Fontaine C, Matthews HK, Kuriyama S, Moreno M, Dunn GA, Parsons M, Stern CD, Mayor R (2008) Contact inhibition of locomotion in vivo controls neural crest directional migration. *Nature* 456(7224):957–961
- Discher D, Janmey P, Wang Y (2005) Tissue cells feel and respond to the stiffness of their substrate. *Science* 310(5751):1139–1143
- Evan G, Vousden K (2001) Proliferation, cell cycle and apoptosis in cancer. *Nature* 411(6835):342–348
- Flaherty B, McGarry JP, McHugh PE (2007) Mathematical models of cell motility. *Cell Biochem Biophys* 49(1):14–28
- Friedl P, Wolf K (2010) Plasticity of cell migration: a multiscale tuning model. *J Cell Biol* 188(1):11–19
- Friedl P, Hegerfeldt Y, Tusch M (2004) Collective cell migration in morphogenesis and cancer. *Int J Dev Biol* 48(5–6, SI):441–449
- Geris L, Liedekerke PV, Smeets B, Tjckens E, Ramon H (2010) A cell based modelling framework for skeletal tissue engineering applications. *J Biomech* 43(5):887–892
- Gracheva M, Othmer H (2004) A continuum model of motility in amoeboid cells. *Bull Math Biol* 66(1):167–193
- Grasso S, Hernandez JA, Chifflet S (2007) Roles of wound geometry, wound size, and extracellular matrix in the healing response of bovine corneal endothelial cells in culture. *Am J Physiol Cell Physiol* 293(4):C1327–C1337
- Hayashi K (2006) Tensile properties and local stiffness of cells. In: Holzapfel GA, Ogden RW (eds) *Mechanics of biological tissue*, chap 10. Springer, Berlin/Heidelberg, pp 137–152
- Helenius J, Heisenberg C-P, Gaub HE, Muller DJ (2008) Single-cell force spectroscopy. *J Cell Sci* 121(11):1785–1791
- Huergo MAC, Pasquale MA, González PH, Bolzán AE, Arvia AJ (2011) Dynamics and morphology characteristics of cell colonies with radially spreading growth fronts. *Phys Rev E* 84(2):021917
- Jamali Y, Azimi M, Mofrad MRK (2010) A sub-cellular viscoelastic model for cell population mechanics. *PLoS ONE* 5(8):e12097
- Kim J-H, Dooling LJ, Asthagiri AR (2010) Intercellular mechanotransduction during multicellular morphodynamics. *J R Soc Interface* 7(3):S341–S350
- Kopacz AM, Liu WK, Liu SQ (2008) Simulation and prediction of endothelial cell adhesion modulated by molecular engineering. *Comput Method Appl Mech Eng* 197(25–28):2340–2352
- Lin Y-C, Tambe DT, Park CY, Wasserman MR, Trepast X, Krishnan R, Lenormand G, Fredberg JJ, Butler JP (2010) Mechanosensing of substrate thickness. *Phys Rev E* 82(4, Part 1):041918
- Lo C, Wang H, Dembo M, Wang Y (2000) Cell movement is guided by the rigidity of the substrate. *Biophys J* 79(1):144–152
- Maruthamuthu V, Sabass B, Schwarz US, Gardel ML (2011) Cell-ECM traction force modulates endogenous tension at cell-cell contacts. *Proc Natl Acad Sci USA* 108(12):4708–4713
- Matsushita M, Wakita J, Itoh H, Watanabe K, Arai T, Matsuyama T, Sakaguchi H, Mimura M (1999) Formation of colony patterns by a bacterial cell population. *Physica A* 274(1–2):190–199
- Newman TJ (2005) Modeling multicellular systems using subcellular elements. *Math Biosci Eng* 2(3):20
- Omelchenko T, Vasiliev J, Gelfand I, Feder H, Bonder E (2003) Rho-dependent formation of epithelial "leader" cells during wound healing. *Proc Natl Acad Sci USA* 100(19):10788–10793
- Palsson E (2001) A three-dimensional model of cell movement in multicellular systems. *Future Gener Comput Syst* 17(7):835–852
- Palsson E, Othmer HG (2000) A model for individual and collective cell movement in dictyostelium discoideum. *Proc Natl Acad Sci USA* 97(19):10448–10453
- Pelham R, Wang Y (1997) Cell locomotion and focal adhesions are regulated by substrate flexibility. *Proc Natl Acad Sci USA* 94(25):13661–13665
- Raeber G, Lutolf M, Hubbell J (2005) Molecularly engineered peg hydrogels: a novel model system for proteolytically mediated cell migration. *Biophys J* 89:1374–1388
- Reinhart-King CA, Dembo M, Hammer DA (2008) Cell-cell mechanical communication through compliant substrates. *Biophys J* 95(12):6044–6051
- Schaller G, Meyer-Hermann M (2007) A modelling approach towards epidermal homeostasis control. *J Theor Biol* 247(3):554–573
- Simpson MJ, Baker RE, McCue SW (2011) Models of collective cell spreading with variable cell aspect ratio: a motivation for degenerate diffusion models. *Phys Rev E* 83(2, Part 1):021901

- Stylianopoulos T, Barocas VH (2007) Volume-averaging theory for the study of the mechanics of collagen networks. *Comput Method Appl Mech Eng* 196(31–32):2981–2990
- Takebayashi T, Iwamoto M, Jikko A, Matsumura T, Enomotoiwamoto M, Myoukai F, Koyama E, Yamaai T, Matsumoto K, Nakamura T, Kurisu K, Noji S (1995) Hepatocyte growth-factor scatter factor modulates cell motility, proliferation, and proteoglycan synthesis of chondrocytes. *J Cell Biol* 129(5):1411–1419
- Tambe DT, Hardin CC, Angelini TE, Rajendran K, Park CY, Serrapicamal X, Zhou EH, Zaman MH, Butler JP, Weitz DA, Fredberg JJ, Trepats X (2011) Collective cell guidance by cooperative intercellular forces. *Nat Mater* 10(6):469–475
- Tijsskens E, Ramon H, De Baerdemaeker J (2003) Discrete element modelling for process simulation in agriculture. *J Sound Vib* 266(3):493–514
- Tranquillo R, Lauffenburger D, Zigmond S (1988) A stochastic-model for leukocyte random motility and chemotaxis based on receptor-binding fluctuations. *J Cell Biol* 106(2):303–309
- Trepats X, Fredberg JJ (2011) Plithotaxis and emergent dynamics in collective cellular migration. *Trends Cell Biol* 21(11):638–646
- Trepats X, Wasserman MR, Angelini TE, Millet E, Weitz DA, Butler JP, Fredberg JJ (2009) Physical forces during collective cell migration. *Nat Phys* 5(6):426–430
- Vermolen F, Gefen A (2012) A semi-stochastic cell-based formalism to model the dynamics of migration of cells in colonies. *Biomech Model Mech* 11:183–195
- Zaman MH, Kamm RD, Matsudaira P, Lauffenburger DA (2005) Computational model for cell migration in three-dimensional matrices. *Biophys J* 89(2):1389–1397
- Zemel A, Rehfeldt F, Brown AEX, Discher DE, Safran SA (2010) Cell shape, spreading symmetry, and the polarization of stress-fibers in cells. *J Phys Condens Matter* 22(19):194110